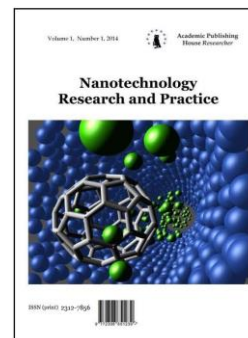


Copyright © 2016 by Academic Publishing House *Researcher*

Published in the Russian Federation
Nanotechnology Research and Practice
Has been issued since 2014.
ISSN: 2312-7856
E-ISSN: 2413-7227
Vol. 12, Is. 4, pp. 109-132, 2016

DOI: 10.13187/nrp.2016.12.109
www.ejournal13.com



Articles and statements

Unsteady MHD Flow and Heat Transfer in *Cu* and *TiO₂* Nanofluid over a Stretchingsheet through a Porous Medium in Presence of Thermal Radiation

Rajnish Kumar ^a, Fauzia Raza ^b, Jahan Akhtar ^c

^a Department of Mathematics, Birla Institute of Technology, Mesra, Patna Campus, Bihar, India
E-mail: rajnish.bitpatna@gmail.com

^b Department of Mathematics, ShriVenkateshwara University, Gajraula, U.P., India
E-mail: rizvi.fauzia786@gmail.com

^c Department of Mathematics, ShriVenkateshwara University, Gajraula, U.P., India
E-mail: jahn4us@yahoo.com

Abstract

This paper deals with the numerical investigation of unsteady flow in a porous medium towards a stretching sheet. Twowater based nanofluids namely *Cu* and *TiO₂* are taken into consideration. With the auxiliary conditions the governing partial differentialequations are converted to ordinary differential equations with the pertinent corresponding conditions. MATLAB function “bvp4c” is applied to solve the resulting governing equations together with the boundary conditions. The effect of various parameters namely: solid volume fractions, Prandtl number, porosity parameter, thermal radiation and the unsteadiness parameter have been discussed. The numerical results obtained for different parameters are presented through plots. Comparison with known results is presented and it is found excellent.

Keywords: nanofluid, Porous Media, Stretching sheet, Thermal radiation, “bvp4c”.

1. Introduction

In nanotechnology the advancements have opened to allow development of a new category of fluids that are termed as nanofluids. A nanofluid is a fluid that refers to contain particles with dimensions less than 100nm. The dispersing medium or in other words the base fluids can be aqueous or non-aqueous in its nature. Oxides, nitrides, carbides or carbon nanotubes are typical nanometer sized particles. Many studies Bhattacharya (Bhattacharya et al., 2004), Mokmeli and Saffar-Avval (Mokmeli, Saffar-Avval, 2010), Mansour (Mansour et al., 2010), Xuan and Li (Xuan, Li, 2000) interpreted that nanofluids apparently display enhanced thermal conductivity, which rises with the increase in volumetric fraction of nanoparticles.

By a porous medium, we mean a material consisting of a solid matrix with an interconnected void. The interconnectedness of the pores allows the flow of one or more fluids through the material. Examples of natural porous are sandstone and limestone. Fluid flow and heat transfer in porous media is a subject of interest for last several decades because of the numerous applications of flow through porous medium, such as storage of radioactive nuclear waste, separation processes in chemical industries, filtration, geothermal extraction, fibre insulation etc. Vafai (Vafai, 2005),

Pop and Ingham (Pop, Ingham, 2001), Ingham and Pop (Ingham, Pop, 1998) and Bejan et al. (Bejan et al., 2004). Yih (Yih, 1999; Yih, 2000) examined coupled heat and mass transfer by free convection over a truncated cone in porous media.

The consequences of thermal radiation may play vital role in controlling heat transfer in industry where the quality of products depend upon heat controlling factors to some extent. The effect of heat transfer problem was discussed by Pal (Pal, 2011). The unsteady MHD free convection flow of an electrically conducting fluid through a porous medium bounded by an infinite vertical and porous plate was explained by Raptis (Raptis, 1986). The dissipative MHD boundary layer flow in a porous medium over a non-linear stretching sheet in the presence of radiation was analysed by Vyas and Ranjan (Vyas, Ranjan, 2010), Wang (Wang, 2008) analyzed two dimensional and axisymmetric stagnation point flow towards a shrinking sheet in viscous fluid. Hiemenz (Hiemenz, 1911) was the first to study the two dimensional stagnation point flow towards a semi-infinite wall. Tiwari and Das (Tiwari, Das, 2007) studied the behaviour of nanofluids by considering the solid volume fraction. Etwire et al. (Etwire et al., 2014) studied the MHD boundary layer stagnation point flow with radiation and chemical reaction towards a heated shrinking porous surface. The effect of MHD stagnation point flow over a porous stretching surface in the presence of radiation and viscous dissipation was studied by Arthur and Seini (Arthur, Seini, 2014). Recently Bachok et al. (Bachok et al., 2010) studied the flow and heat transfer in an incompressible viscous fluid near the three dimensional stagnation point of a body that is placed in water based nanofluid. Choi (Choi, 1995) was the first to utilized nanofluid concepts. He showed that the addition of a small amount of nanoparticles to conventional heat transfer liquid increased the thermal conductivity of the fluid up to two times approx. The effect of free convective heat transfer from a vertical surface to a saturated porous medium with an arbitrary varying surface temperature was analyzed by Gorla and Zinolabedini (Gorla, Zinolabedini, 1987). The physical features namely viscoelasticity of the fluid, suction and three dimensional flow and magnetic field was studied by Takhar and Nath (Takhar, Nath, 1997). The Hankel-Padeexpansion method to study nanofluid MHD boundary layer flows was used by Abbasbandy and Ghehsareh (Abbasbandy, Ghehsareh, 2012). Kuznetsov and Geng (Geng, Kuznetsov, 2005) analysed the effect of solid particles in a dilute suspension containing gyrolactic micro-organism.

The aim of the present work was to analyze the effect of thermal radiation on boundary layer flow of a nanofluid over a stretching sheet with an unsteady free stream condition. The effects owe to uncertainties of thermal conductivity and dynamic viscosity has been analyzed.

2. Mathematical formulation

2.1. Governing equations

Consider the unsteady two-dimensional boundary layer flow due to a stretching sheet in a fluid. The fluid is a water based nanofluids containing two types of nanoparticles such as Copper and Titanium. It is also assumed that the base fluid and nanoparticles are in thermal equilibrium and no slip occurs between them. The thermo-physical properties of regular fluid and nanoparticles are given in Table 1.

Table 1. The thermo-physical properties of regular fluid and nanoparticles

Physical properties	Regular fluid(water)	Copper(Cu)	Titanium (TiO ₂)
c _p (J/kg K)	4179	385	686.2
ρ(kg/m ³)	997.1	8933	4250
k (W/mK)	0.613	400	8.9538

The governing equations of the present problem are

$$\frac{\partial u}{\partial x} + \frac{\partial v}{\partial y} = 0 \tag{1}$$

$$\frac{\partial u}{\partial t} + u \frac{\partial u}{\partial x} + v \frac{\partial u}{\partial y} = \frac{\mu_{nf}}{\rho_{nf}} \frac{\partial^2 u}{\partial y^2} - \frac{v_{nf}}{K_1} u - \frac{\sigma B^2(x)}{\rho_{nf}} u \tag{2}$$

$$\frac{\partial T}{\partial t} + u \frac{\partial T}{\partial x} + v \frac{\partial T}{\partial y} = \alpha_{nf} \frac{\partial^2 T}{\partial y^2} - \frac{1}{(\rho c_p)_{nf}} \frac{\partial q_r}{\partial y} \tag{3}$$

where u and v are velocity components along the axes x and y respectively, ν_{nf} is the kinematic viscosity, μ_{nf} is the dynamic viscosity of the nanofluid, T is the temperature, ρ_{nf} is the density of the nanofluid, $(\rho C_p)_{nf}$ is the heat capacity of the nanofluid, α_{nf} is the thermal diffusivity with, c_p is the heat capacity at constant pressure and q_r is the radiative heat flux

$$\begin{aligned} \rho_{nf} &= (1 - \phi)\rho_f + \rho_s, \quad \mu_{nf} = \frac{\mu_f}{(1-\phi)^{2.5}} \cdot \alpha_{nf} = \frac{k_{nf}}{(\rho C_p)_{nf}} \\ (\rho C_p)_{nf} &= (1 - \phi)(\rho C_p)_f + (\rho C_p)_s, \quad \frac{k_{nf}}{k_f} = \frac{(k_s + 2k_f) - 2\phi(k_f - k_s)}{(k_s + 2k_f) + \phi(k_f - k_s)} \end{aligned} \quad (4)$$

where ϕ is the solid volume fraction. k_{nf} is the thermal conductivity of the nanofluid. k_s is the thermal conductivity of solid fractions and k_f is the thermal conductivity of base fluid The radiative heat flux under rosseland approximation (Brewster, 1992) has the form:

$$q_r = -\frac{4\sigma}{3k_1} \frac{\partial T^4}{\partial y}, \quad (5)$$

where k_1 and σ are the mean absorption coefficient and the Stefan-Boltzman constant.

We assume that the temperature difference within the flow is sufficiently small such that T^4 can be expressed as a linear function of temperature. Hence expanding T^4 in Taylor series about T_∞ and neglecting higher order terms, we get

$$T^4 \cong 4T_\infty^3 - 3T_\infty^4 \quad (6)$$

Using equations (5) and (6), equation (3) reduces to:

$$\frac{\partial T}{\partial t} + u \frac{\partial T}{\partial x} + v \frac{\partial T}{\partial y} = \alpha_{nf} \frac{\partial^2 T}{\partial y^2} + \frac{16\sigma T_\infty^3}{3k_1 \rho c_p} \frac{\partial^2 T}{\partial y^2} \quad (7)$$

2.2. Boundary conditions

The corresponding boundary conditions are:

$$\begin{aligned} u &= U_w(x,t), \quad v = 0, \quad T = T_w(x,t), \quad C = C_w(x,t) \text{ at } y = 0 \\ u &\rightarrow U(x), \quad T \rightarrow T_\infty, \quad C \rightarrow C_\infty \text{ at } y \rightarrow \infty. \end{aligned} \quad (8)$$

T_w is the surface temperature and T_∞ is the temperature of the fluid outside the boundary layer. Following Ishak et al. (Ishaq et al., 2009), the stretching velocity is considered as

$$U_w(x,t) = \frac{ax}{1-at} \quad (9)$$

where a and c are constants (with $a \geq 0, \alpha \geq 0$ such that $at < 1$) and both have dimension t^{-1} .

We have a as the initial stretching rate $\frac{a}{1-at}$ and it increases with time. We considered the surface temperature $T_w(x,t)$ the stretching sheet to vary with the distance x and an inverse law for its decrease with time as:

$$T_w = T_\infty + \frac{bx}{(1-at)^2} \quad (10)$$

2.3. Non-dimensionalization

Now introducing the following similarity transformations

$$\begin{aligned} \eta &= \left(\frac{b}{v}\right)^{1/2} (1 - at)^{-1/2} y, \quad \psi = (bv)^{1/2} (1 - at)^{-1/2} x F(\eta) \\ \theta(\eta) &= \frac{T - T_\infty}{T_w - T_\infty} \end{aligned} \quad (11)$$

where ψ is the stream function that satisfies Eq.(1) with

$$u = \frac{\partial \psi}{\partial y} \text{ and } v = -\frac{\partial \psi}{\partial x} \quad (12)$$

In terms of these variables the velocity components can be expressed as,

$$u = \frac{ax}{1-at} F'(\eta), \quad v = -\sqrt{\frac{av_f}{1-at}} F(\eta) \quad (13)$$

The transformed momentum, energy and mass diffusion equations together with the boundary conditions given by (1)-(8) reduced to:

$$F'''' - (1 - \phi)^{2.5} \left\{ 1 - \phi + \phi \frac{\rho_s}{\rho_f} \right\} \left[A \left(F' + \frac{1}{2} F'' \eta \right) + F'^2 - FF'' + MF' \right] = 0 \quad (14)$$

$$\theta'' + \frac{1}{(1+Nr)} Pr \frac{k_{nf}}{k_f} \left\{ 1 - \phi + \phi \frac{(\rho c p)_s}{(\rho c p)_f} \right\} \left[F\theta' - F'\theta - A(2\theta + \frac{\eta}{2}\theta') \right] = 0 \tag{15}$$

And $F'(0) = \varepsilon, \theta(0) = 1, \text{ at } \eta = 0$

$F'(0) = 1, \theta(0) = 0, \text{ at } \eta = 0$ (16)

Where $Pr = \frac{\nu_f}{\alpha_f}$ is the Prandtl number, $Nr = \frac{kk_1}{4\sigma T_\infty^3}$ is the parameter of radiation, $M = \frac{\sigma B_0^2}{\alpha \rho_{nf}} + \frac{\nu_{nf}}{\alpha K_0}$ is the combined magnetic and porosity parameter and $A = \frac{\alpha}{b}$ is dimensionless measure of the unsteadiness. $\varepsilon = \frac{a}{b}$ is the velocity ratio parameter.

2.4. Physical quantities of engineering interest

The physical quantities of interest are the skin friction coefficient and the local Nusselt number which are defined a

$$C_f = \frac{\mu}{\rho_f U_w^2} \left(\frac{\partial u}{\partial y} \right)_{y=0}$$

$$Nu = \frac{x}{k(T_W - T_\infty)} \left[k \left(\frac{\partial T}{\partial y} \right)_{y=0} - \frac{4\sigma}{3k_1} \left(\frac{\partial T^4}{\partial y} \right)_{y=0} \right] \tag{17}$$

With μ and k are the dynamic viscosity and thermal conductivity, respectively. Using non-dimensional variables (12), we have

$$C_f Re_x^{1/2} = F''(0), \frac{Nu_x}{Re_x^{1/2}} = -\theta''(0), \tag{18}$$

3. Method of solution

The sets of equations (15)-(17) with boundary conditions (18) constitute a two-point boundary value problem. These equations are solved using “bvp4c” function of MATLAB software package. “bvp4c” is a finite difference code that implements Lobattolla formula and the collocation polynomials allocate a C¹-continuous solution that is fourth-order accurate uniformly in the interval of integration. Mesh selection and error control are based on residual of the continuous solution.

The collocation method uses a mesh of points to divide the interval of integration into subintervals. The solver ascertains a numerical solution by solving a global system of algebraic equations resulting from the boundary conditions, and the collocation conditions imposed on each subinterval. The solver then estimates the error of the numerical solution on each subinterval. If the solution does not satisfy the tolerance criteria, the solver adapts the mesh and repeats the procedure.

4. Results and discussion

For the validation of the study, the case when the unsteadiness and porosity parameter is absent has been also considered and compared with the results reported by Mahapatra and Gupta (Mahapatra, Gupta, 2002) and Nazar et al. (Nazar et al., 2004). This comparison is shown in Table 2.

Table 2. Comparisons of the values of $F''(0)$ for various values of ε

	Mahapatra and Gupta	Nazar et al.	Present work
ε	$-F''(0)$	$-F''(0)$	$-F''(0)$
0.2	-0.9181	-0.9181	-0.918107
0.5	-0.6673	-0.6673	-0.667262
2.0	2.0175	2.0176	2.017416
3.0	4.7293	4.7296	4.567275

Table 3 and Table 4 shows computational values of $-F''(0)$ and $-\theta'(0)$ for Copper and Titanium nanoparticles with different values of ϕ From Table 3, it is clear that the value of $-F''(0)$ is minimum at $\phi = 0.5$ for both the nanofluids.

Table 3. Values of $-F''(0)$ and $-\theta'(0)$ for different values of ϕ when $A=0.1$, $M=0.2$, $\varepsilon =1$, $Nr=0.12$ and $Pr=1$

ϕ	$-F''(0)$		$-\theta'(0)$	
	<i>Cu</i>	<i>TiO₂</i>	<i>Cu</i>	<i>TiO₂</i>
0.0	0.88999	0.88999	1.07122	1.07122
0.1	1.05447	0.89843	0.99231	0.91656
0.2	1.09153	0.86532	0.67673	0.79438
0.3	1.05762	0.80081	0.56479	0.69503
0.4	0.96160	0.71182	0.52574	0.61297
0.5	0.83461	0.60352	0.45473	0.54298

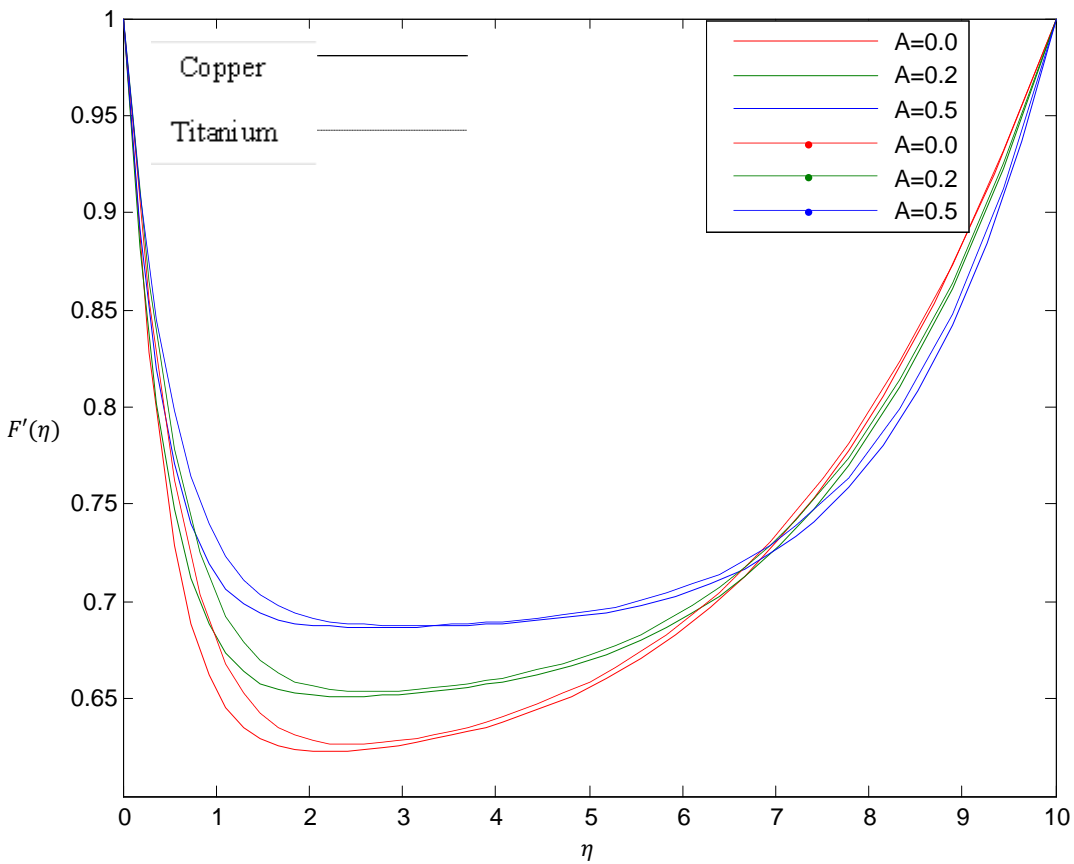


Fig. 1. $\phi=0.2$, $M=1$, $\varepsilon=1$, $A=0.0, 0.2, 0.5$. Velocity profile for different values of unsteadiness parameter A

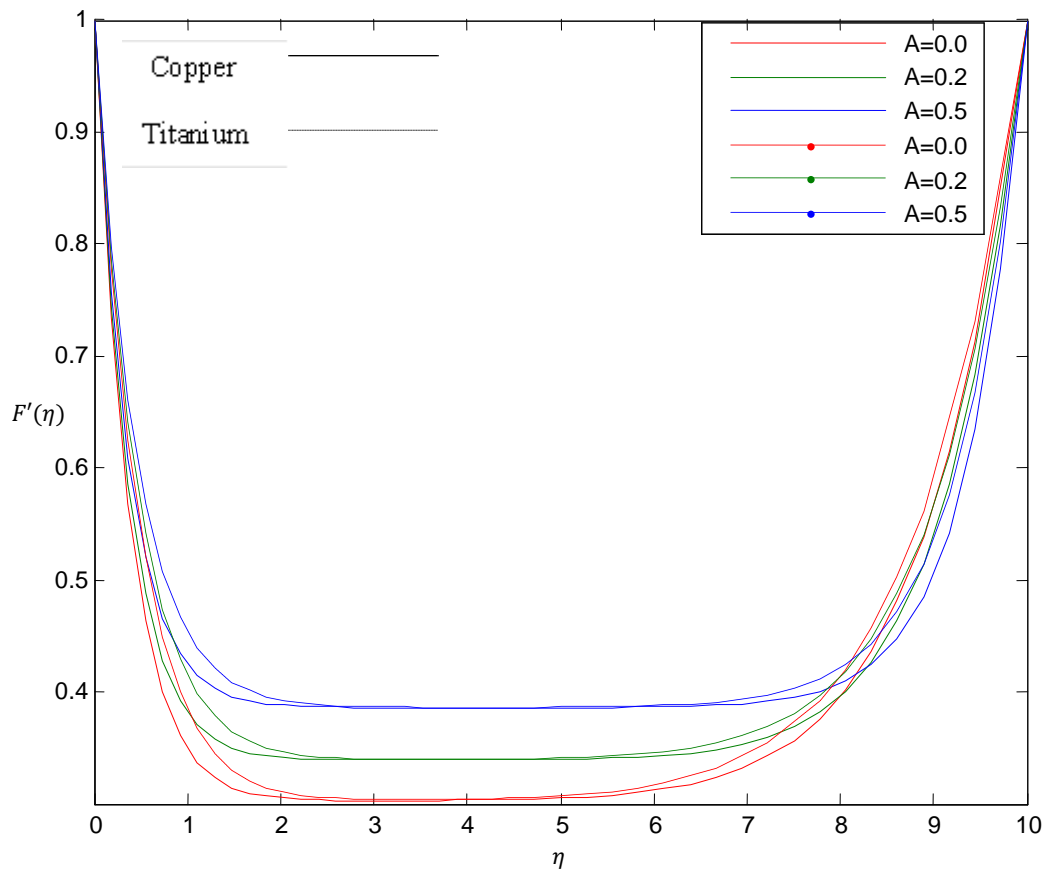


Fig. 2. $\phi=0.2$, $M=3$, $\epsilon=1$, $A=0.0, 0.2, 0.5$. Velocity profile for different values of unsteadiness parameter A

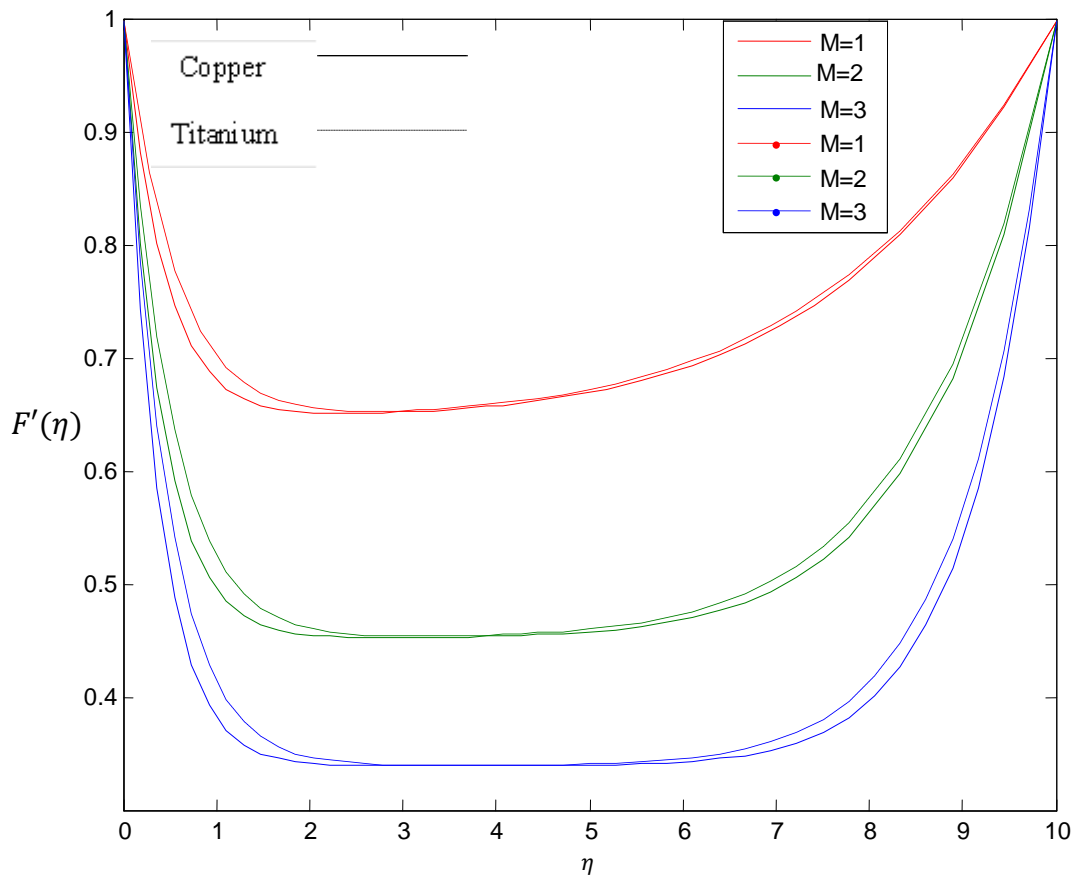


Fig. 3. $M=1, 2, 3, \phi=0.2, A=0.2, \epsilon=1$. Velocity profile for different values of combined magnetic and porosity parameter M

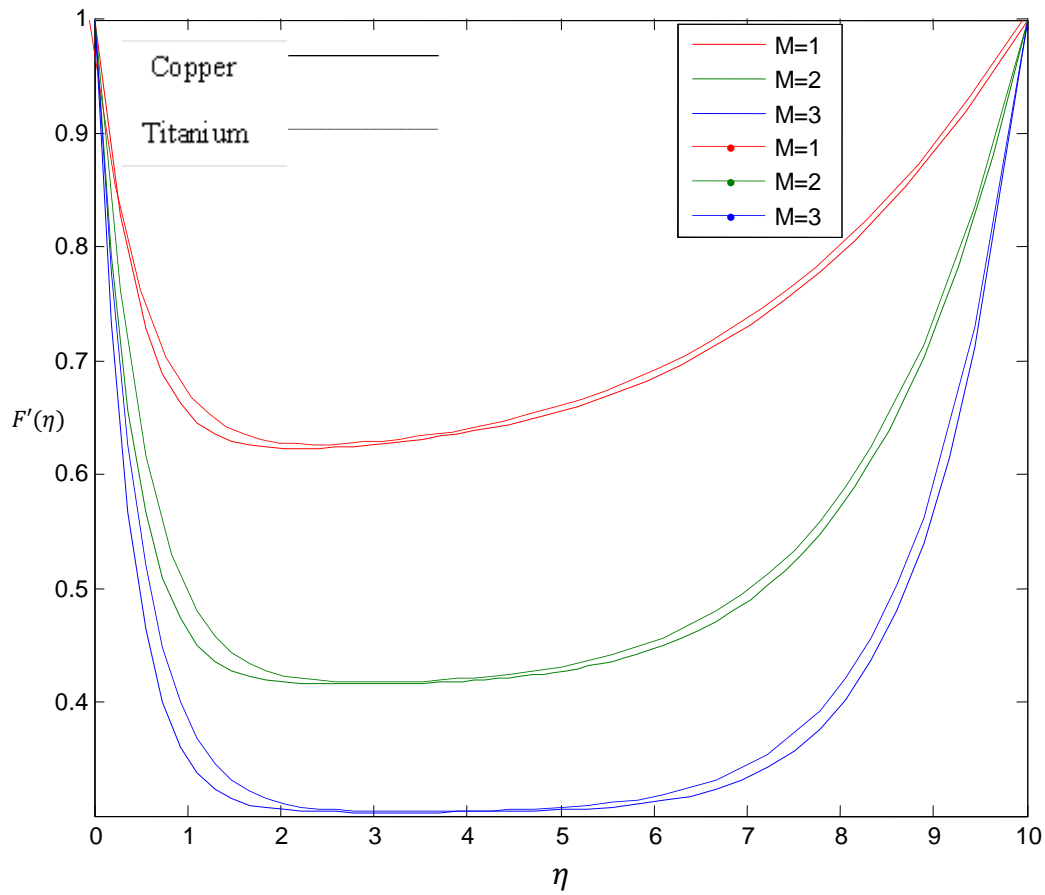


Fig. 4. M=1, 2, 3, $\phi= 0.2$, $A=0.0$, $\epsilon=1$. Velocity profile for different values of combined magnetic and porosity parameter M

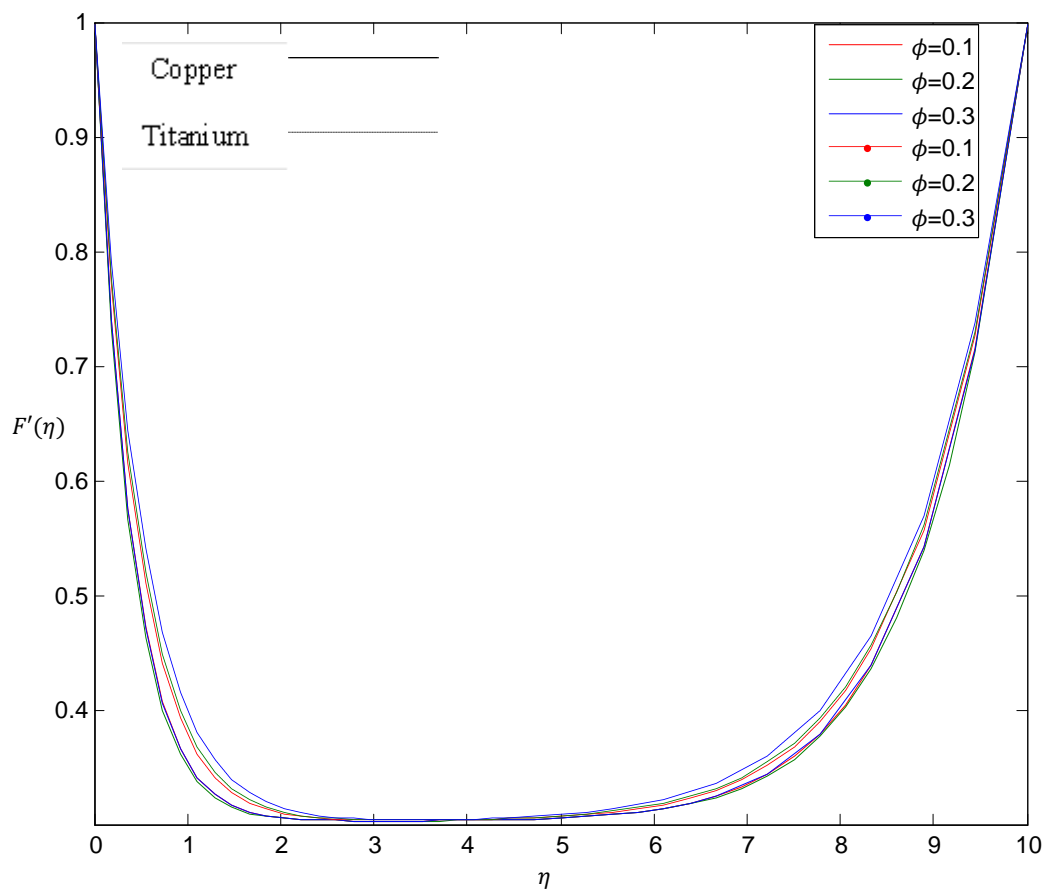


Fig. 5. $\phi=0.1, 0.2, 0.3, A=0.0, M=3, \epsilon=1$. Velocity profile for different values of solid volume fraction ϕ

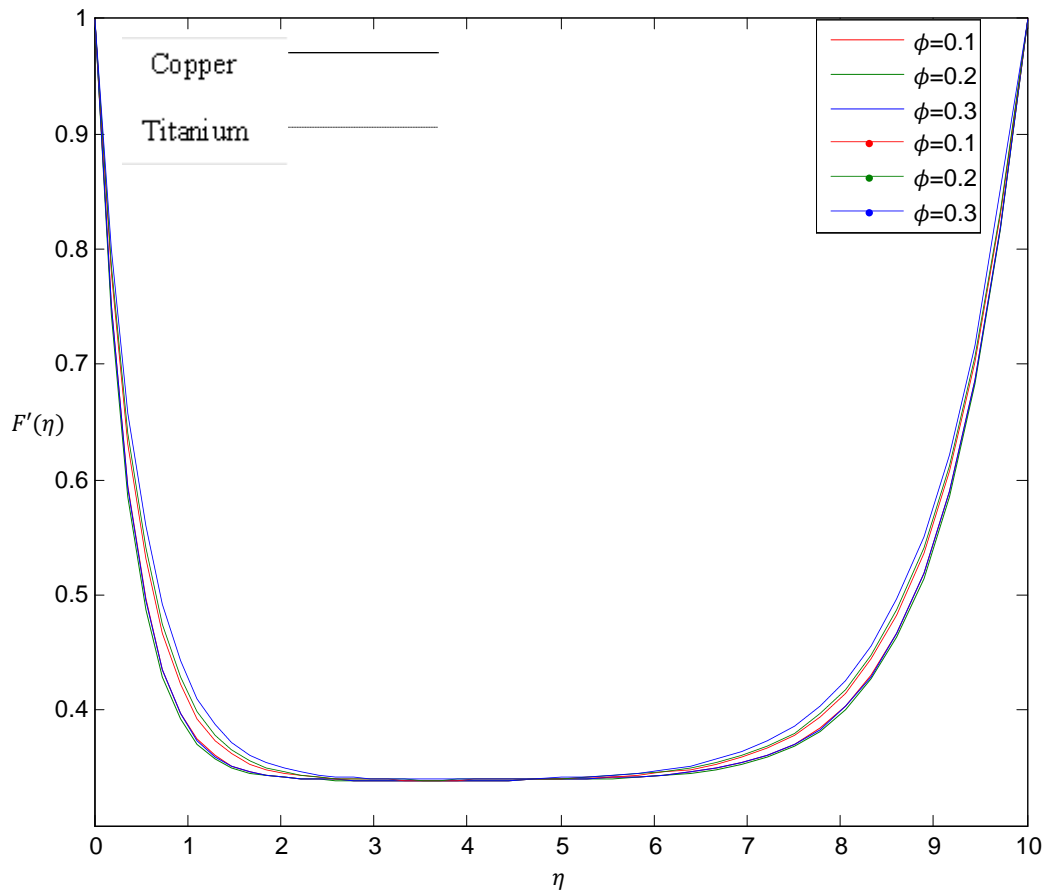


Fig. 6. $\phi=0.1, 0.2, 0.4, A=0.2, M=3, \epsilon=1$. Velocity profile for different values of solid volume fraction ϕ

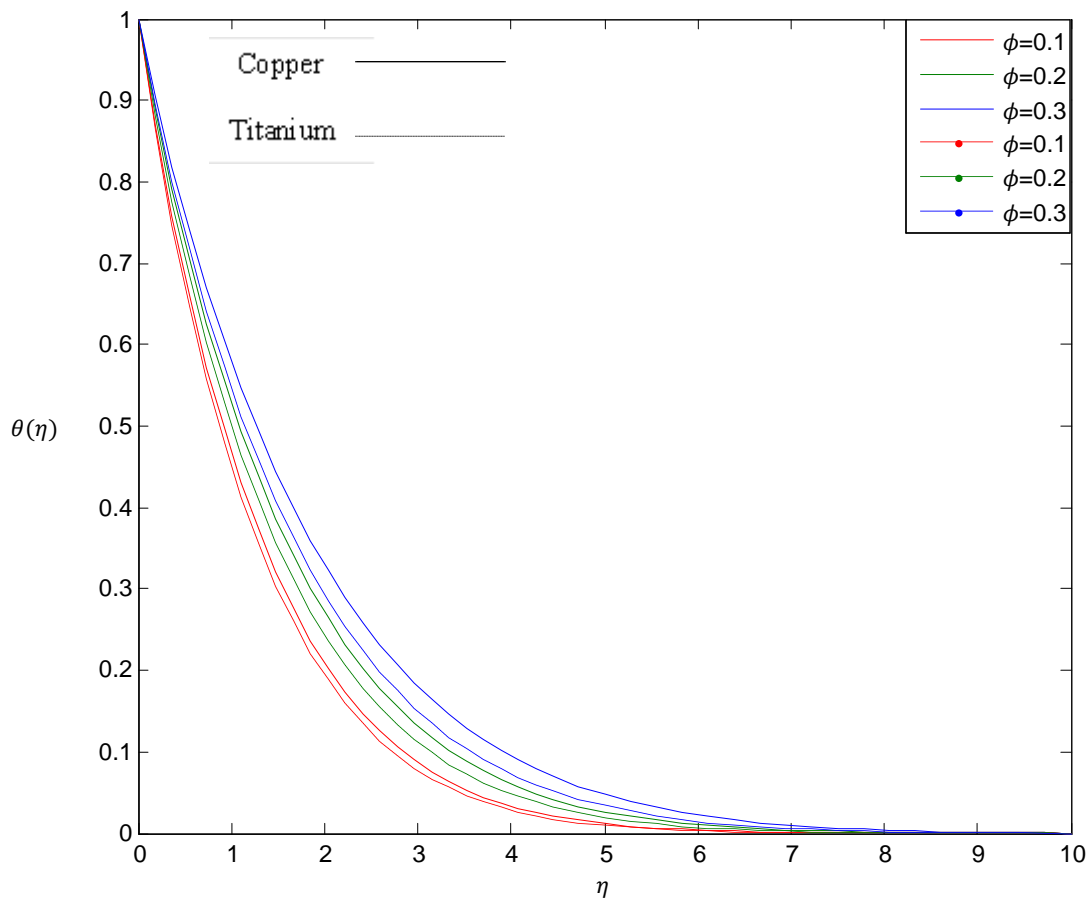


Fig. 7. $\phi=0.1, 0.2, 0.3, A=0.2, Pr=0.72, Nr=0.12$. Temperature profile for different values of solid volume fraction ϕ

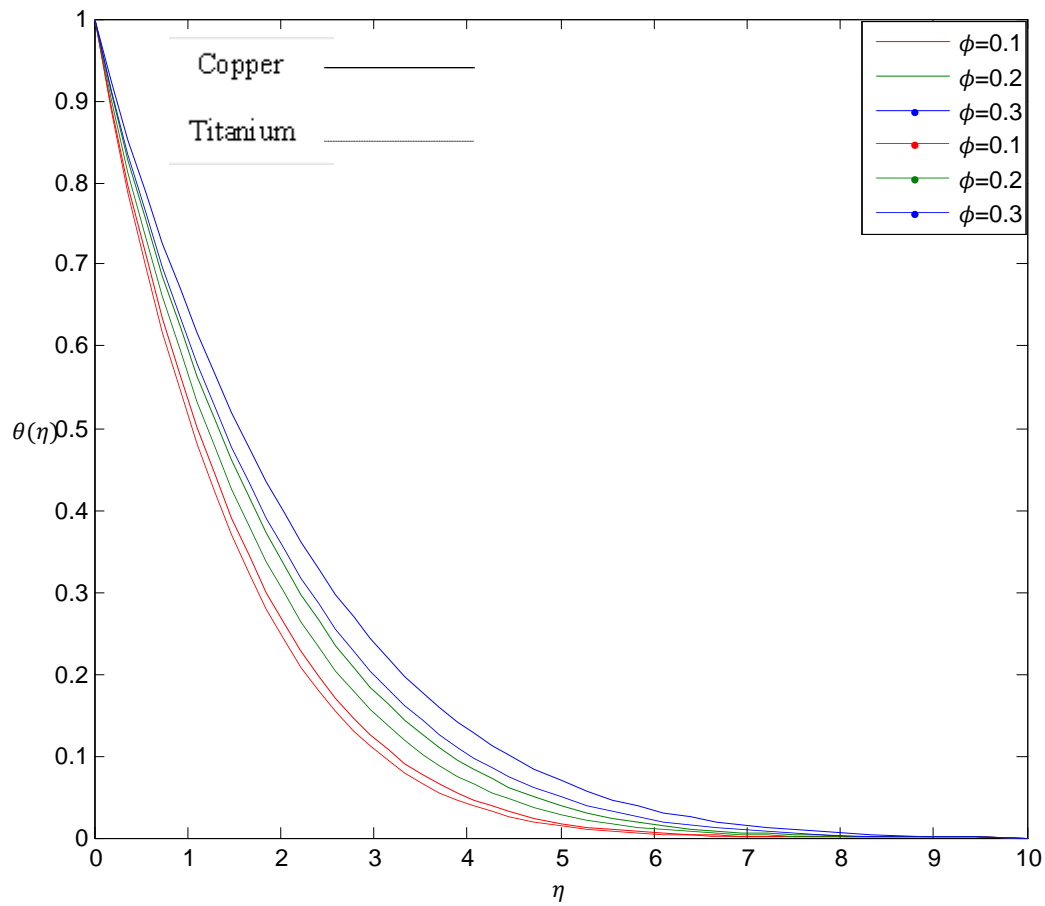


Fig. 8. $\phi=0.1, 0.2, 0.3, A=0.0, Pr=0.72, Nr=0.12$. Temperature profile for different values of solid volume fraction ϕ

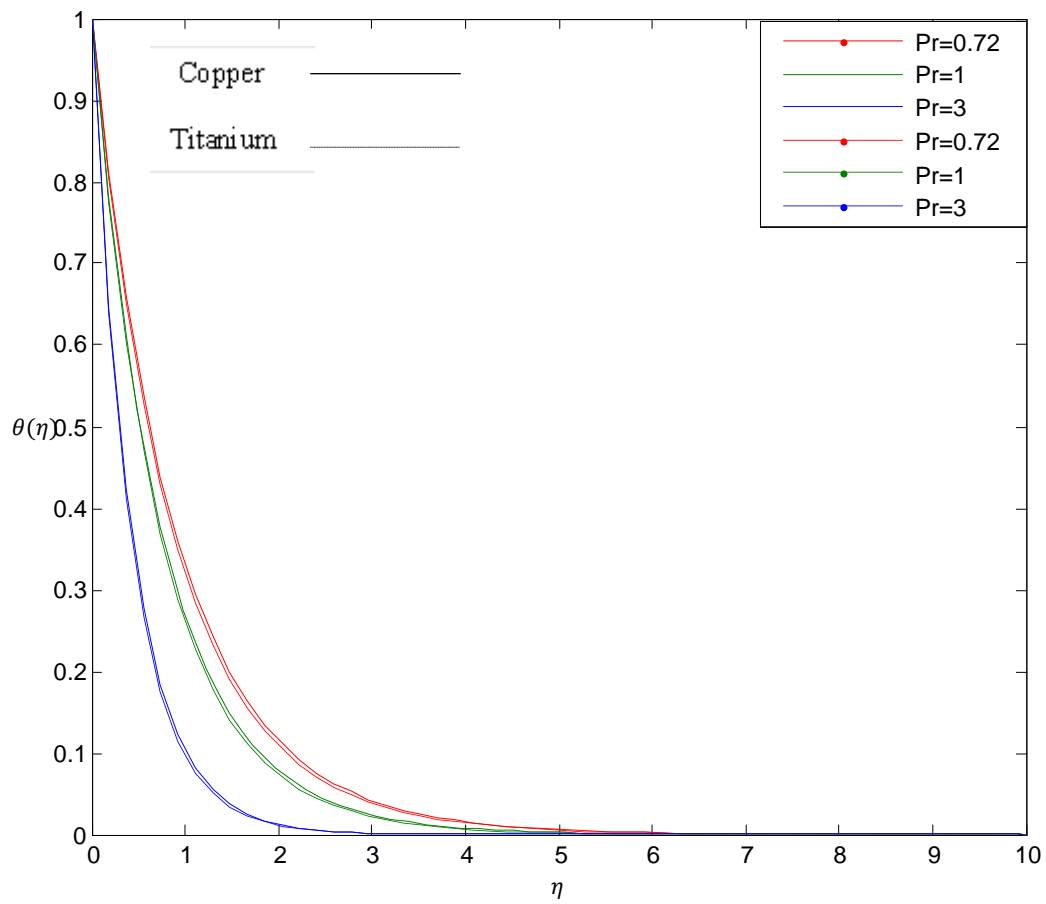


Fig. 9. $Pr=0.72, 1, 3, Nr=0.5, A=1.5, \phi=0.1$. Temperature profile for different values of Prandtl number Pr

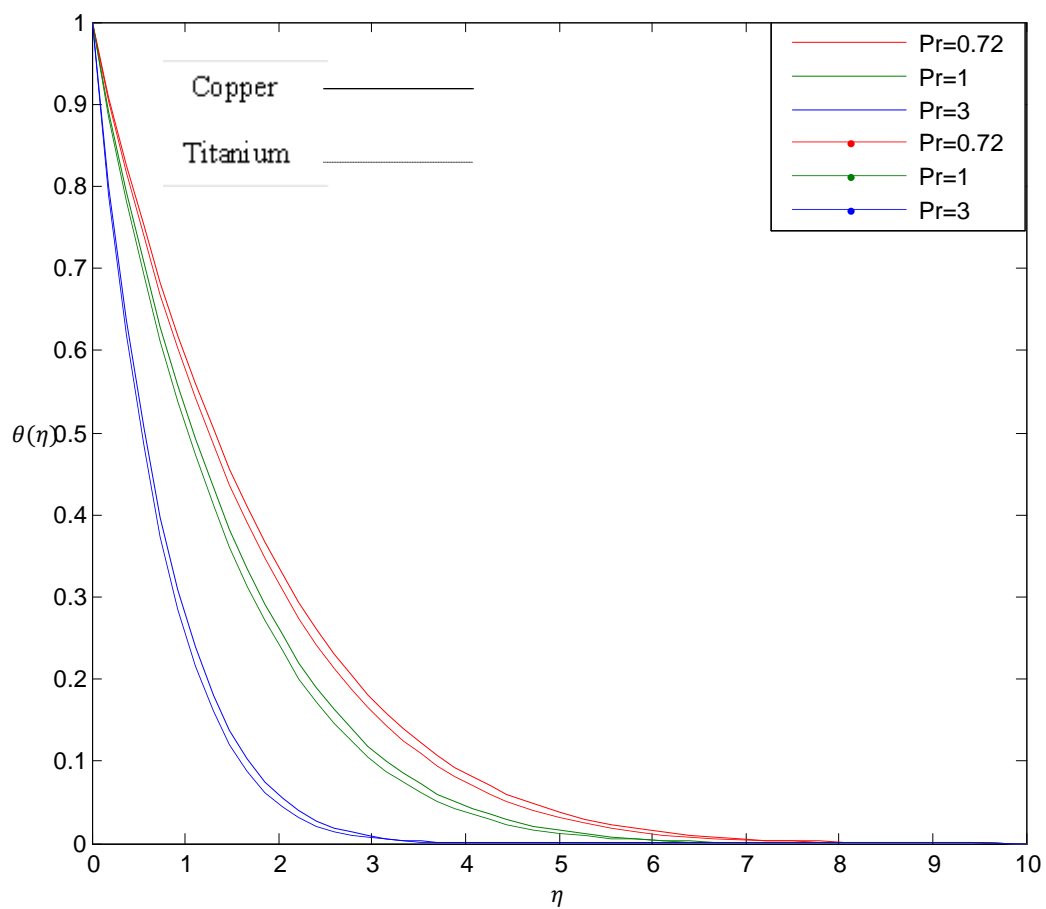


Fig. 10. $Pr=0.72, 1, 3, Nr=0.5, A=0.0, \phi=0.1$. Temperature profile for different values of Prandtl number Pr

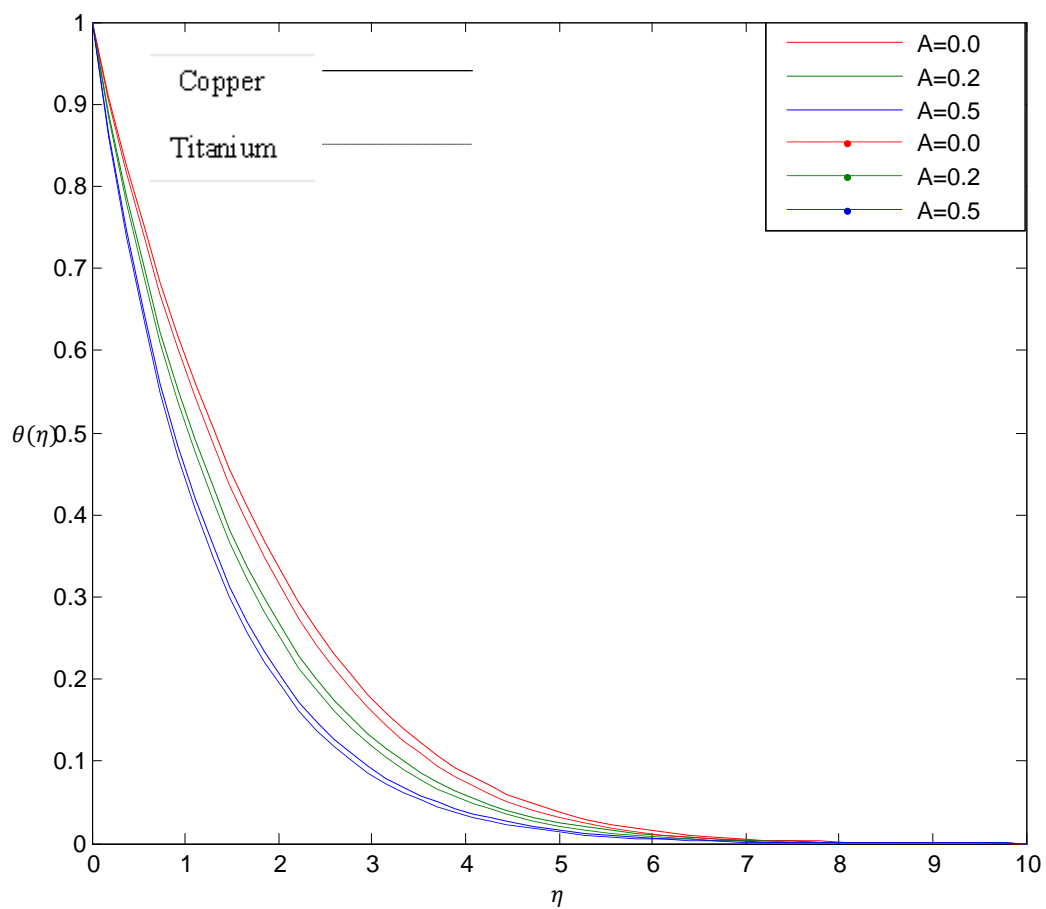


Fig. 11. $Nr=0.5$, $Pr=0.72$, $A=0.0, 0.2, 0.5$, $\phi=0.1$. Temperature profile for different values of unsteadiness parameter A

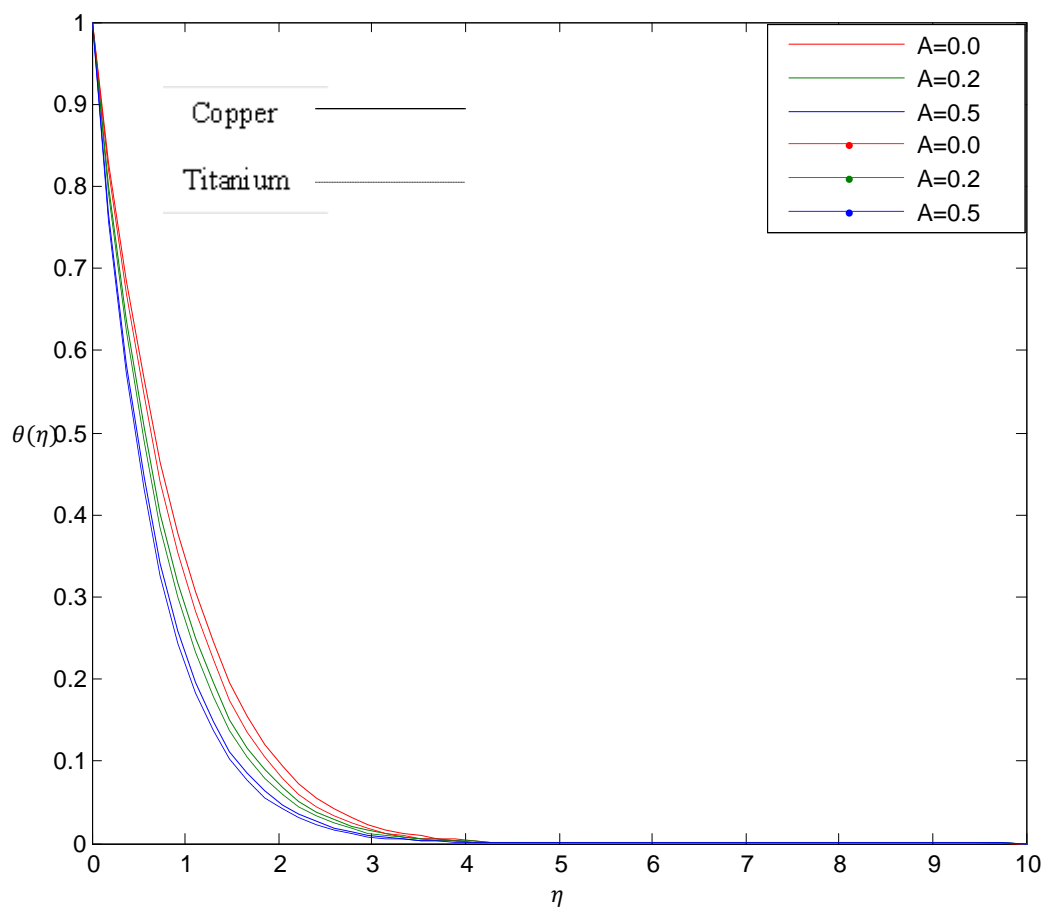


Fig. 12. $Nr=1$, $Pr=3$, $A=0.0, 0.2, 0.5$, $\phi=0.1$, Temperature profile for different values of unsteadiness parameter A

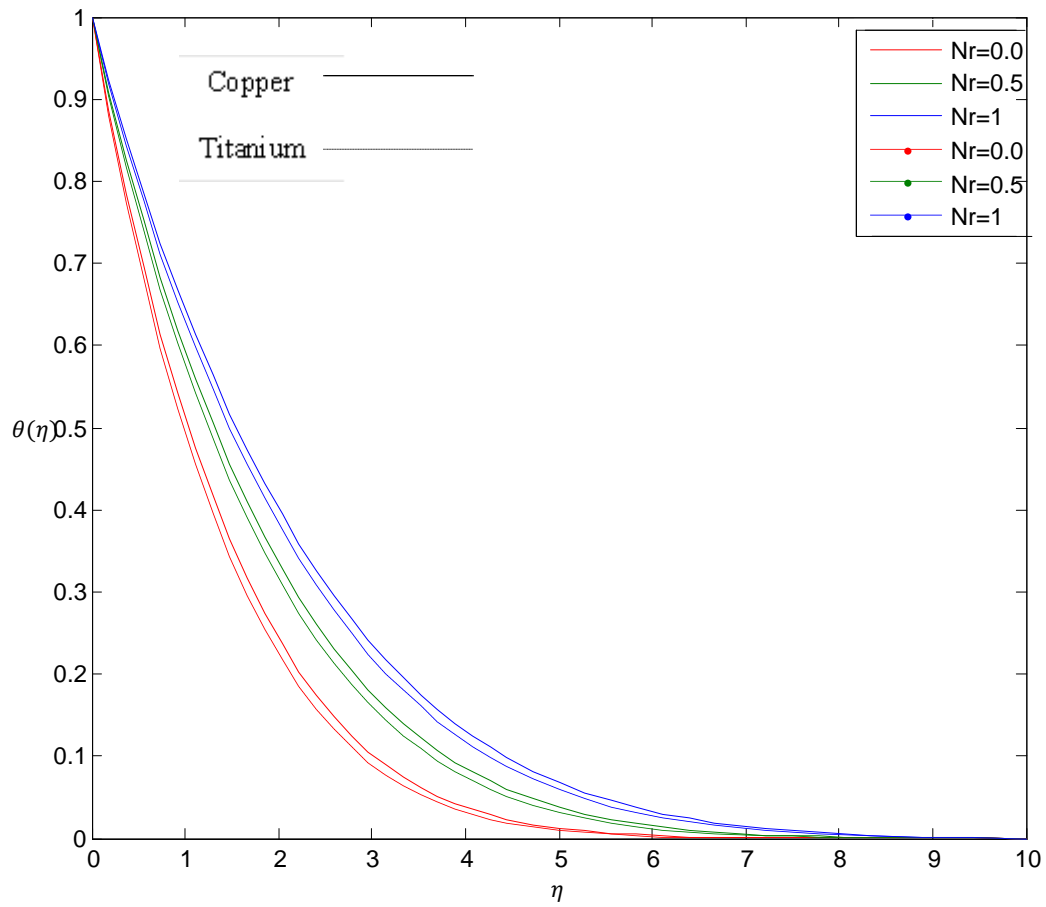


Fig. 13. $A=0.0$, $Pr=0.72$, $Nr=0.0, 0.5, 1$, $\phi=0.1$. Temperature profile for different values of radiation parameter Nr

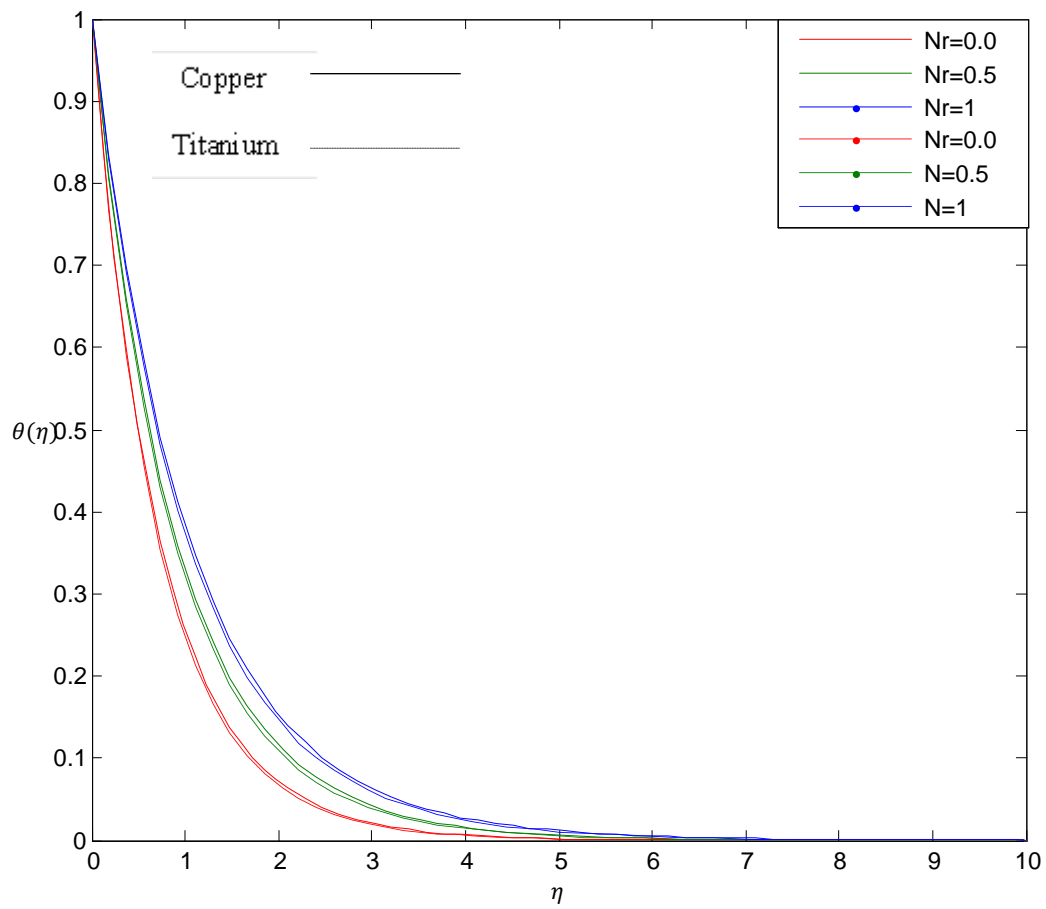


Fig. 14. $A=1.5, P=0.72, Nr=0.0, 0.5, 1, \phi=0.1$. Temperature profile for different values of radiation parameter Nr

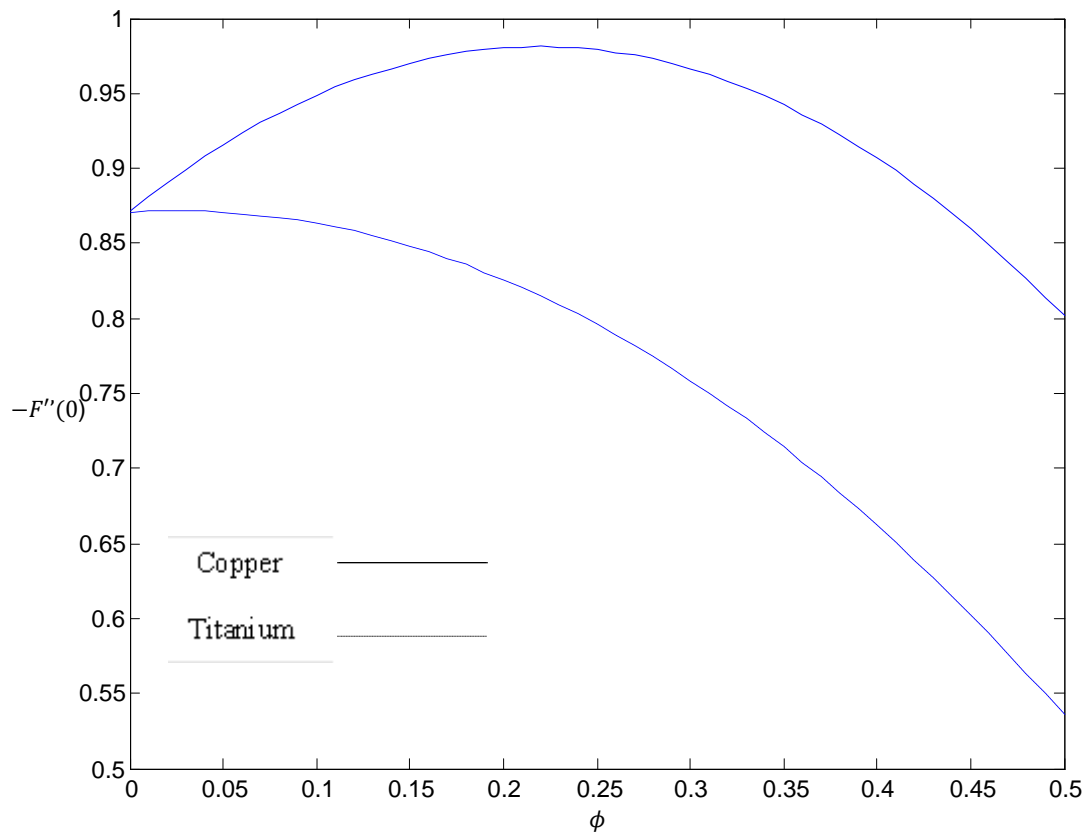


Fig. 15. Pr=6.25, M=3, Nr=0.12, A=0.0. Skin friction against different values of ϕ

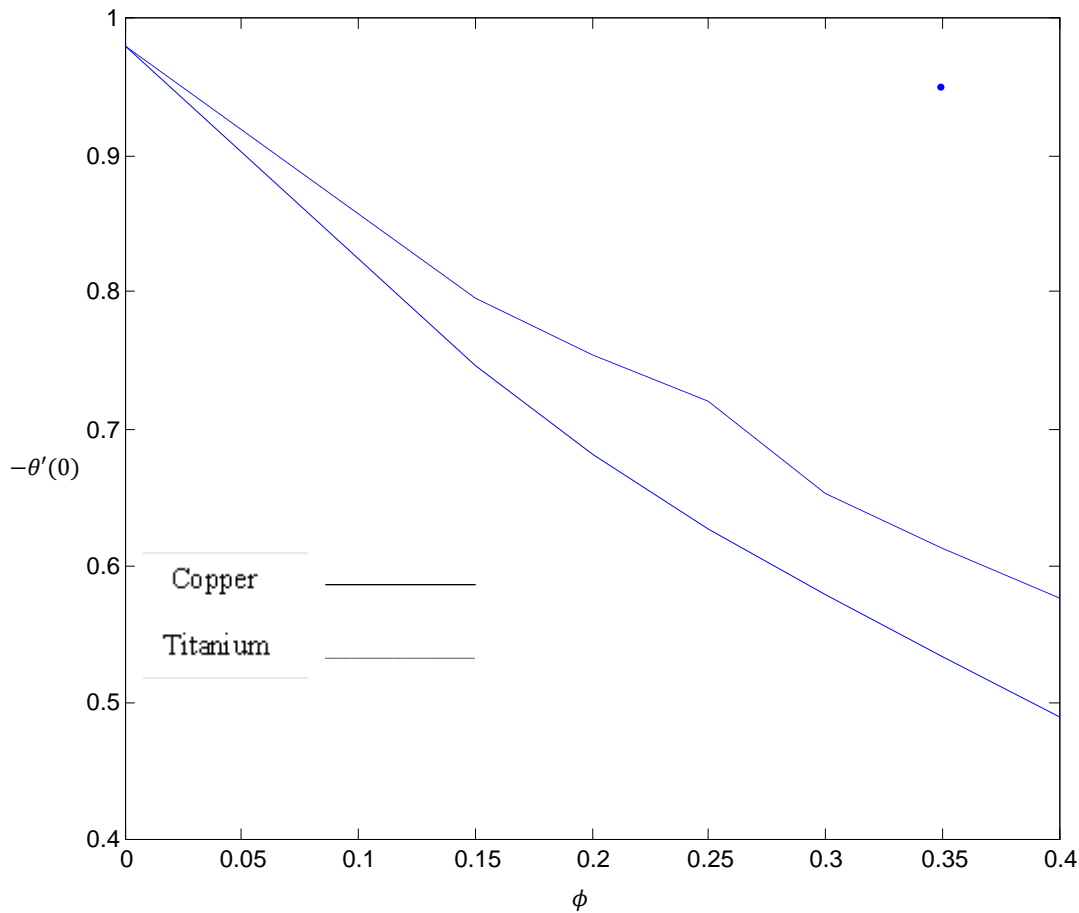


Fig. 16. Pr=6.25, M=3, Nr=0.12, A=0.0. Nusselt number against different values of ϕ

4.1. Effect of parameter variation on the velocity profile:

The velocity profile for varying parameters is shown in Fig. 1-6. Fig. 1 and Fig. 2 are the profile of unsteadiness parameter A. Fig. 1 depicts the variation in A when $\phi = 0.2, M = 1$ and Fig. 2 presents the variation in A when $\phi = 0.2, M = 3$. From Fig. 1 and 2 it is obvious that the velocity profile for unsteadiness parameter A is decreasing to a certain level and again it is increasing. In Fig. 1 the velocity profile decreases and it is minimum for A=0.0 and in Fig. 2 the velocity profile is minimum for A=0.0 for both the nanoparticles. Fig. 3 and Fig. 4 are for combined magnetic and porosity parameter M. Fig. 3 shows that when $\phi = 0.2, A = 0.2$ the velocity profile is decreasing and it is minimum for $M = 3$ and again it increases. Fig. 4 shows that when $\phi = 0.2, A = 0.0$ the velocity profile is decreasing and again it tends to 1.

The volume fraction ϕ is for Fig. 5 and fig. 6. In Fig. 5, we consider the steady state i.e. $A = 0.0, M = 3$; it shows that the velocity profile is decreasing and it is minimum at 0.0 and again it increases to 1. Fig. 6 shows that when $A = 0.2, M = 3$, the velocity profile decreases to 0.2 and again it increases asymptotically to 1.

Table 4. Values of $-F''(0)$ and $-\theta'(0)$ for different values of ϕ when $A=0.0$, $M=0.2$, $\epsilon =1$, $Nr=0.12$ and $Pr=1$

ϕ	$-F''(0)$		$-\theta'(0)$	
	Cu	TiO_2	Cu	TiO_2
0.0	0.86066	0.86066	0.97970	0.97970
0.2	0.99364	0.84198	0.68061	0.75380
0.3	0.96123	0.73301	0.57823	0.65309
0.4	0.88057	0.65133	0.48955	0.57618
0.5	0.81931	0.55195	0.14871	0.51099

4.2. Effect of parameter variation on temperature profile:

Fig. 7-14 presents the temperature profile for different parameters. Fig. 7 and Fig. 8 are for variation in solid volume fractions ϕ . From the figs it is obvious that the thermal boundary layer thickness increases continuously with the volume fraction of nanoparticles. This happens due to the presence of solid nano-particles which leads to further thinning of the velocity boundary layer thickness.

Fig. 9 and Fig. 10 are the temperature profiles for Prandtl number Pr for fixed values of A and R . The Prandtl number is a dimensionless number, defined as the ratio of momentum diffusivity to thermal diffusivity. There is a decrease in temperature with increase in Prandtl number. This is because of the fact that there would be decrease of thermal boundary layer thickness with the increase of Prandtl number.

Fig. 11 and Fig. 12 are the temperature profiles for unsteadiness parameter A . From Fig. 11 and fig12 it is obvious that the temp profiles decreases with the increase in unsteadiness parameter A and the thermal boundary layer thickness decreases with increase in unsteadiness parameter A . Fig. 13 and Fig. 14 are the temperature profiles for radiation parameter Nr for steady and unsteady flow respectively. The fig itself shows that for a fixed value of A and Pr the profile of temperature is decreased with the increasing Nr . It is also observed that the boundary layer thickness increases with the increase in value of Nr . Fig. 15 and Fig. 16 are for variation in $-F''(0)$ and $-\theta'(0)$ against ϕ for variant thermo-physical properties of water and nanoparticles.

5. Conclusion

In this paper, the consequences of unsteady fluid flow over a stretching sheet in presence of thermal radiation in porous media have been analyzed. The investigation is performed for variant mentioned parameters and some conclusions are summarized as follow:

- The thermal boundary layer thickness decreases with increase in Prandtl number.
- The present result has been compared with Mahapatra and Gupta (Mahapatra, Gupta, 2002) and Nazar (Nazar et al., 2004). The consistency between the results is admirable.
- The local Nusselt number is maximum for all the nanofluids at $\phi = 0.0$.
- The effect of radiation parameter on temperature distribution is found to be more noticeable at greater unsteadiness parameter.

Acknowledgements

The authors would like to thank UGC, Govt. of India for the financial supports under UGC Start-Up-Research Grant No.F.20-1(19)/2012(BSR).

References

Abbasbandy, Ghehsareh, 2012 – Abbasbandy, S, Ghehsareh, HR (2012). Solutions of the magnetohydrodynamic flow over a nonlinear stretching sheet and nano boundary layers over stretching surfaces. *Int J Number Methods Fluids*, 70: 1324–1340.

- Arthur, Seini, 2014 – Arthur, E.M., Seini I.Y. (2014). Hydromagnetic Stagnation Point Flow over a Porous Stretching Surface in the Presence of Radiation and Viscous Dissipation. *Applied and Computational Mathematics*, 3(5): 191-196.
- Bachok et al., 2010 – Bachok, N, Ishak, A, Nazar, R, Pop, I (2010). Flow and heat transfer at a general three dimensional stagnation point flow in a nanofluid. *Physica B*, 405: 4914-4918.
- Bejan et al., 2004 – Bejan, A, Dincer, I, Lorente, S, Miguel, AF, Reis, AH (2004). Porous and complex flow structures in modern technologies. Springer, New York.
- Bhattacharya et al., 2004 – Bhattacharya, P, Saha, S, Yadav, A, Phelan, P, Prasher, R. (2004). Brownian dynamics simulation to determine the effect of thermal conductivity of nanofluids. *J. Appl. Phys.* 95: 6492-6494.
- Brewster, 1992 – Brewster, MQ (1992). Thermal Radiative Transfer Properties, Wiley, Canada.
- Choi, 1995 – Choi, SUS (1995). Enhancing thermal conductivity of fluids with nanoparticles. In: Siginer DA, Wang HP (eds). Development and applications of non-Newtonian flows. ASME MD, vol. 231 and FED, vol. 66. USDOE, Washington, DC: 99-105.
- Etwire et al., 2014 – Etwire, C.J., Seini, Y.I., Arthur, E.M. (2014). MHD Boundary Layer Stagnation Point Flow with Radiation and Chemical Reaction towards a Heated Shrinking Porous Surface, *International Journal of Physical Science*, 9(14): 320-328.
- Geng, Kuznetsov, 2005 – Geng, P, Kuznetsov, AV (2005). Settling of bidispersed small solid particles in a dilute suspension containing gyrotactic microorganisms. *Int. J. Eng. Sci*, 43: 992–1010.
- Gorla, Zinolabedini, 1987 – Gorla, RSR, Zinolabedini, A (1987). Free convection from a vertical plate with non-uniform surface temperature embedded in a porous medium. *ASME J Energy Res Technol*, 109: 26–30.
- Hiemenz, 1911 – Hiemenz, K (1911). Die Grenzschicht an einem in den gleichförmigen Flüssigkeitsströmeingetauchtgeraden Kreiszyylinder. *Dingler's Polytech J*, 326: 321-324.
- Ingham, Pop, 1998 – Ingham, DB, Pop, I (1998). Transport phenomena in porous media, vol I. Pergamon, Oxford, vol II, 2002.
- Ishaq et al., 2009 – Ishaq, A, Nazar R, Pop, I (2009). Boundary layer flow and heat transfer over an stretching vertical surface. *Meccanica*, 44: 1-14.
- Mahapatra, Gupta, 2002 – Mahapatra, TR, Gupta, AS (2002). Heat transfer in stagnation-point flow towards a stretching sheet. *Heat and Mass Transf*, 38: 517-521.
- Mansour et al., 2010 – Mansour, M, Mohamed, R, Abd-Elaziz, M, Ahmed, S (2010). Numerical simulation of mixed convection flows in a square lid-driven cavity partially heated from below using nanofluid. *Int. Commun. Heat Mass transfer*, 37: 1504-1512.
- Mokmeli, Saffar-Avval, 2010 – Mokmeli, A, Saffar-Avval M, (2010). Prediction of nanofluid convective heat transfer using the dispersion model. *Int. J. Therm. Sci*, 49: 471-478.
- Nazar et al., 2004 – Nazar, R, Amin, N, Filip, D, Pop, I (2004). Unsteady boundary layer flow in the region of the stagnation point on a stretching sheet. *Int J Eng Sci*, 42: 1241-1253.
- Pal, 2011 – Pal, D (2011). Combined effects of non-uniform heat source/sink and thermal radiation on heat transfer over a stretching permeable surface. *Commun Nonlinear Sci. Number. Simulat.*, 16: 1890-1904.
- Pop, Ingham, 2001 – Pop, I, Ingham, DB (2001). Convective heat transfer: mathematical and computational modelling of viscous fluids and porous media. Pergamon, Oxford.
- Raptis, 1986 – Raptis, AA (1986). Flow through a porous medium in the presence of a magnetic field. *Int. J Energy Res*, 10: 97-100.
- Takhar, Nath, 1997 – Takhar, HS, Nath, G (1997). Similarity solution of unsteady boundary layer equations with a magnetic field. *Meccanica*, 32: 157-163.
- Tiwari, Das, 2007 – Tiwari, RK, Das, MK (2007). Heat transfer augmentation in a two-sided lid-driven differentially heated square cavity utilizing nanofluids. *Int J Heat Mass Transfer*, 50: 2002-2018.
- Vafai, 2005 – Vafai, K (2005). Handbook of porous media, 2nd edn. Taylor & Francis, New York.

Vyas, Ranjan, 2010 – Vyas, P, Ranjan, A (2010). The dissipative MHD boundary-layer flow in a porous medium over a sheet stretching nonlinearly in the presence of radiation. *Applied Mathematical Sciences*, 4(63): 3133-3142.

Wang, 2008 – Wang CY (2008). Stagnation flow towards a shrinking sheet. *Int J Non Lin Mech*, 43: 377-382.

Xuan, Li, 2000 – Xuan, Y, Li, O (2000). Heat transfer enhancement ofnanofluids. *Int. J. Heat Fluid Flow*, 21: 58-64.

Yih, 1999 – Yih, KA (1999). Coupled heat and mass transfer by free convection over a truncated cone in porous media: VWT/VWC or VHF/VMF. *ActaMech*, 137: 83–97.

Yih, 2000 – Yih, KA (2000). Combined heat and mass transfer in mixed convection adjacent to a VWT/VWC or VHF/VMF cone in a porous medium: the entire regime. *J Porous Media*, 3(2): 185–191.